Optica Applicata, Vol. XL, No. 4, 2010

Noise reduction for digital holograms in a discrete cosine transform (DCT) domain

HYUN-JUN CHOI[1*], YOUNG-HO SEO[2], DONG-WOOK KIM[2]

[1]Anyang University, 708-113, Anyang-5Dong, Manan-Gu, Anyang-Shi, Kyonggi-Do 430-714, Republic of Korea

[2]Kwangwoon University, 447-1, Welgye-1Dong, Nowon-Gu, Seoul 139-701, Republic of Korea

[*]Corresponding author: hjchoi@anyang.ac.kr

This paper presents a method for reducing noise in a digital hologram, which occurs during acquisition. The algorithm proposed initially transforms a digital hologram into frequency-domain data through a discrete cosine transform (DCT), and separates the object from the background in the transformed image. As a noise reduction method, a histogram modification method is applied to the object, while the background is substituted with zero values. Experimental results showed that the proposed scheme improves the visual image quality very much when reconstructed by both the optical system and the PC simulation.

Keywords: digital hologram, noise reduction, discrete cosine transform (DCT), holographic reconstruction.

1. Introduction

Holography is regarded as the optimal and the final choice for imaging and displaying three-dimensional (3D) objects. Recently, with the help of advanced mega-pixel CCD sensors that have a sufficient dynamic range in each pixel, digital holography has become a viable 3D imaging technique [1]. Therefore, the interference pattern is captured in digital format by a CCD sensor and the object is displayed by loading the stored digital hologram on an SLM (spatial light modulator). The noise is intruded in the process of acquiring the interference pattern due to the environments relating to the camera and its characteristics. The noise lowers the quality of the reconstructed hologram, but increases the entropy of the digital hologram, which makes the signal process of the hologram such as data compression less efficient [2–7].

The technique of removing noise from a natural image has long been experimented, and, consequently, many noise-removing filters showing superior performances have been designed. However, these filters are not suitable for a digital hologram because the noise has similar frequency band to the original image data. Some studies [8, 9] proposed the noise-removing techniques for the digital hologram using those image processing techniques. In [10], a method using a wavelet filter has been proposed.

These techniques expanded the applicability of the methods to the 2-dimensional (2D) images corresponding to digital holograms.

The digital hologram has a characteristic that each pixel has a very low correlation to other pixels, which is very similar to a noise. In this paper, a new approach to remove or reduce the noise in a digital hologram is proposed, which uses a frequency transform to increase the correlation among the pixels. A 2D discrete cosine transform (2DDCT) is used as the transform tool. The distribution in the frequency-domain coefficients resembles the one of the reconstructed images [11]. Therefore the object and the background are separated in the transformed domain, each of them being analyzed to propose a different noise-removing/reduction technique.

In Section 2, the characteristics of a digital hologram are analyzed. Section 3 explains the noise-removing/reduction method proposed in this paper with a brief review of some previous ones. The experimental results are provided with some discussion in Section 4, and Section 5 concludes the paper.

2. Analysis of digital hologram

In general, a digital hologram is acquired by capturing with a CCD camera the phase of interference pattern generated by the reference light and the object light (reflected from an object) and recorded in a digital format, as shown in Fig. 1**a**. In the figures, M_1, M_2, and M_3 are the mirrors, BE and BS represent beam expander and beam splitter, respectively, and L_1 and L_2 are the lenses. Therefore, a digital hologram shows substantially different characteristics from a natural image which shows self--similarity, the foundation of fractal theory, and strong correlation between adjacent pixels in an image (refer to Figs. 2**a** and 2**b**). However, a digital hologram is much more irregular, uncorrelated, and discontinuous so that it looks very similar to a noise, as shown in Figs. 2**c** and 2**d**.

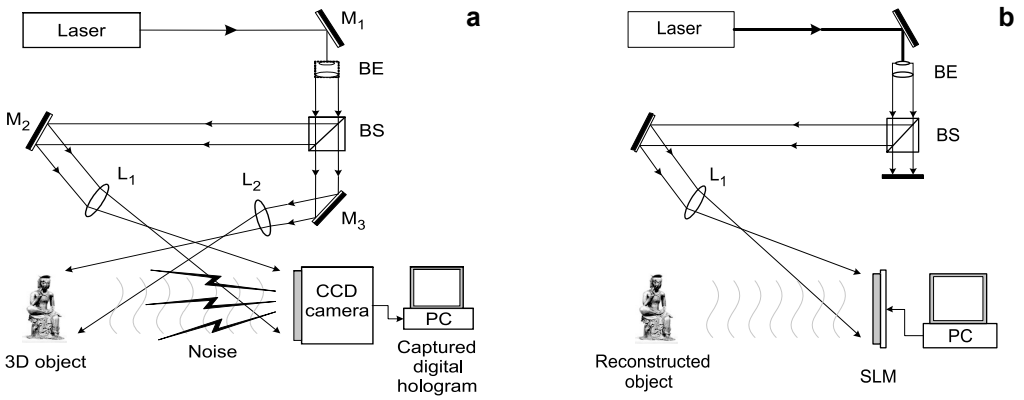

Fig. 1. Acquisition (**a**) and reconstruction (**b**) scheme of digital hologram.

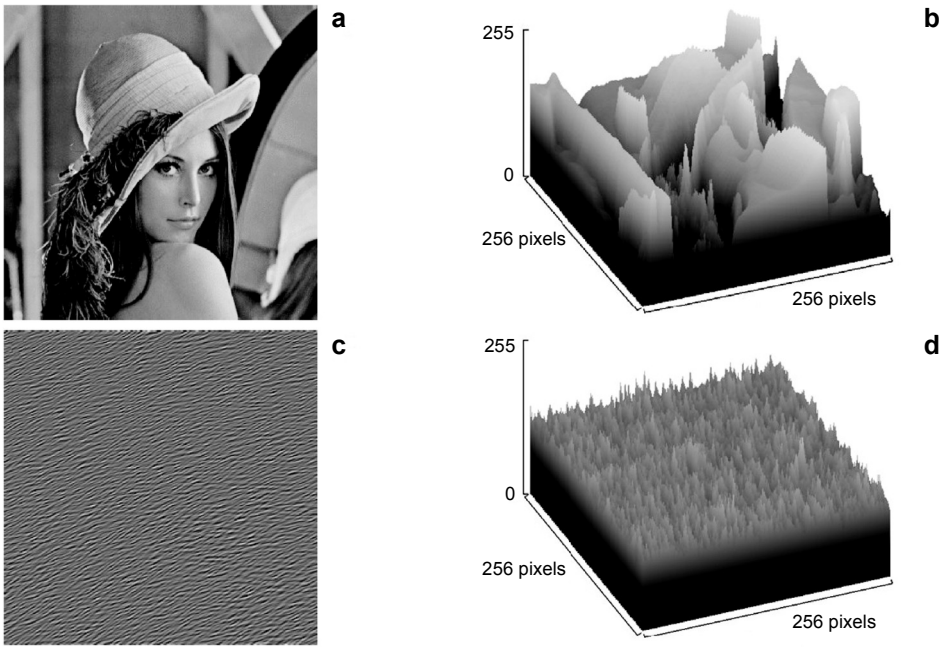

Fig. 2. Example images; natural image (**a**), positional pixel values of **a** (**b**), digital hologram (**c**), positional pixel values of **c** (**d**).

Figure 1**b** also shows a reconstruction scheme of an object. To reconstruct the object the same light wave as the reference one used in acquisition should be irradiated to the digital hologram at the same distance as in acquisition. Because a digital hologram is stored in a digital form, it is uploaded to a special equipment named SLM, in general.

The use of CCD camera in the acquisition process of a digital hologram inherently includes some noises because of the environments of camera, and they dramatically decrease the quality of reconstructed images. Thus, it is highly required to remove or reduce such noise from the hologram domain. Because of the differences in its characteristics from a conventional 2D image, the methods of removing or reducing noise for a 2D image are inappropriate and cannot be expected to give us an acceptable performance. By considering them, this paper proposes a noise reduction algorithm for a digital hologram, which uses transformation with 2DDCT as a tool for transforming a digital hologram into its frequency domain data.

The reason for using the 2DDCT is that it reconstructs the object from the digital hologram to a reasonable degree and the result is quite proper to apply our noise reduction algorithm. Because a digital hologram can be constructed by applying the Frensnel transform, it could be better to use the inverse Fresnel transform to reconstruct the object, but it takes much more time compared with 2DDCT. The Fourier

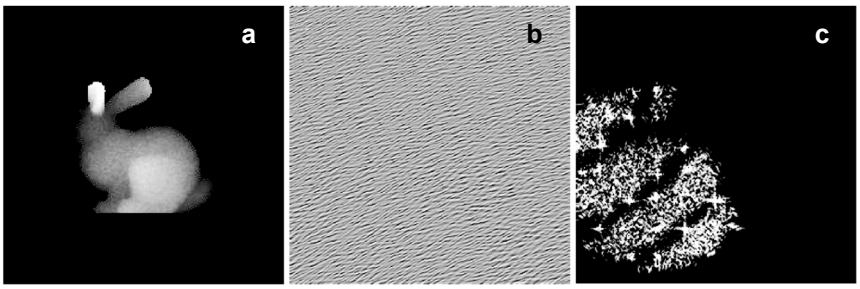

Fig. 3. Depth-map image of 3D object (**a**), digital hologram of **a** with dimensions of 256×256 (**b**), GDCT result of **b** (**c**).

transform can also be considered as the transformation, but it shows much lower image quality than 2DDCT, although the execution time is similar to 2DDCT.

This paper applies 2DDCT to the whole digital hologram without dividing it, which we call the global DCT (GDCT) [12], and which can be expressed as

$$S(u, v) = \frac{C(u)C(v)}{2} \sum_{x=0}^{M-1} \sum_{y=0}^{N-1} s(x, y) \cos\left[\frac{(2x+1)u\pi}{2M}\right] \cos\left[\frac{(2x+1)u\pi}{2N}\right] \tag{1}$$

$$C(u), C(v) = \begin{cases} \sqrt{\frac{1}{2}} & u, v = 0 \\ 1 & \text{otherwise} \end{cases}$$

where the digital hologram is assumed to have the size of $M \times N$, and $S(u, v)$ and $s(x, y)$ are the transformed and original pixel values at (u, v) and (x, y), respectively. Figure 3 shows an example of the GDCTed image, where (**a**) is a depth-map of the image (200×200 [pixel^2]), (**b**) is its digital hologram (256×256 [pixel^2]), and (**c**) is the result from GDCT of (**b**). It can be figured out that the GDCT result quite well resembles the original object although its position is somewhat different. One particular result from this example is that the value of transformed DC coefficient from a digital hologram does not seem to be so high. But digital hologram still have very high values and energies even though they are lower than that for a conventional 2D image.

3. The proposed noise reduction algorithms

In this section, we propose a noise reduction algorithm for digital hologram. It is briefly shown in Fig. 4, in which the solid lines depict the algorithm while the dashed lines are to experiment the performance. In this figure, the gray block, *noise addition* step is to generate the noisy digital holograms and it is not part of the noise reduction technique, that is, the real input for noise reduction is the *noisy digital hologram*.

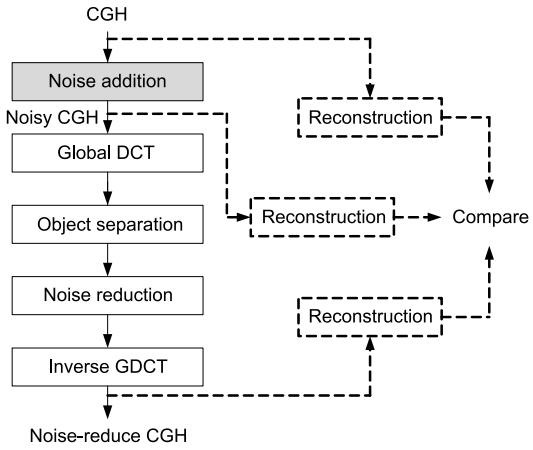

Fig. 4. Block diagram of the whole algorithm and experimental scheme.

The reason why this block is inserted is to explain how we perform the noise modeling and the experiments. Each component of our algorithm is explained in this section and the experiment is dealt with in the next section. For computer-generated hologram (CGH), we give explanation in the following section.

3.1. Computer-generated hologram (CGH)

The acquisition method of a digital hologram in Fig. 1 can be applied in very restricted cases or places, where all the equipment as well as the CCD camera are prepared. Therefore, a more convenient method has been researched and it is called as computer--generated hologram (CGH) [13]. As its name suggests, it calculates the interference pattern by the two light waves: reference wave and object wave (Eq. (2)), and it is also known as Fresnel transform

$$I_\alpha = \sum_{j=0}^{Q-1} A_j \cos(\theta_H + \Phi_\alpha + \Phi_j)$$
$$\theta_H = k R_{\alpha j} = k\sqrt{(px_\alpha - px_j)^2 + (py_\alpha - py_j)^2 + z_j^2} \tag{2}$$

In this equation, I_α is the hologram intensity at position $\alpha = (x_\alpha, y_\alpha)$ by summing up all the influences from the object to α by all the light sources at $j = (x_j, y_j, z_j)$ (Q is the number of light sources). Here, $k = 2\pi/\lambda$ is the wave number of the reference wave, where λ is its wavelength, p is the pixel pitch of the hologram, and A_j is the light intensity of the light source at j.

Equation (2) only needs 3D location and light intensity of each light source, which are luminance and depth of the light source, and can be obtained from Y component of the YCbCr color format and the depth map, respectively. Therefore, CGH is much more convenient to acquire and is the one to be used in this paper as well.

3.2. Noise model

The digital hologram acquired as Fig. 1 is different from CGH in that taking a picture with a CCD camera itself includes some noise caused by several factors as explained before. That is, a CGH is the interference pattern itself without any noisy component. Thus it is quite general to consider some noise related to data transmission as well as the one related to acquisition.

Let us consider the acquisition situation of Fig. 1. The image acquisition itself in Fig. 1 shows no differences from that of acquiring a 2D image. Also, considering the service model (acquisition, coding, transmission, receiving, decoding, and display) for hologram service, the transmission noise in this case is not much different from that for a 2D image/video. Consequently, if we want to use CGH as the target hologram, it is necessary to consider the acquisition noise and transmission noise for which we can use a model applied to 2D images.

Many investigations have been conducted for noises caused by acquisition and transmission for 2D image/video and the representative one is to add some Gaussian noise [14]. We also use this noise model for digital hologram service, which is depicted in Fig. 5. As mentioned above, a CGH $h(i, j)$ is obtained by calculation using Eq. (2) with intensities and depths of the object light sources. Then a Gaussian noise $n(i, j)$ is added to form a noisy digital hologram h,

$$h'(i, j) = h(i, j) + n(i, j) \tag{3}$$

where the Gaussian noise has the average at 0 and the standard deviation σ^2.

3.3. Noise reduction techniques for conventional 2D images

The existing noise removing/reduction algorithms targeting on natural 2D images use linear filter(s) and non-linear filter(s). An averaging filter and/or a Gaussian filter are usually used as linear filters [14]. Although implementation of these filters is fairly easy, they show a defect of blurring at the edges, corners, and high frequency areas such as textures. To improve the artifacts by linear filters, non-linear filter(s) are additionally used. A median filter [14] is a representative one, which sorts and changes the pixel values into the median value. A sigma filter [15] diminishes the deduced noise by changing its value into the average value in a situation where the difference between the surrounding pixels and the central pixel is less than the predefined threshold value. Also, a non-linear filter named AWA (adaptive weight average)

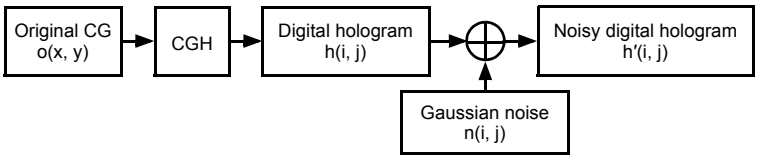

Fig. 5. Noise model for digital hologram service.

filter [14] has been proposed, where the weight value varies relative to the difference between the surrounding pixel values and the central pixel value. The influence of such non-linear filters on the high frequency components is less significant than that of linear filters. But still they might induce blurring phenomena as filtering intensity increases.

Those noise reduction algorithms are for conventional 2D images, where the low--frequency components are dominant and the high-frequency components seem to be aggregated in some particular areas. Because a hologram has much different characteristics so that its pixel correlations are considerably low and the high-frequency components are distributed all around the images, as shown in Figs. 2**c** and 2**d**, they do not work properly for a hologram.

3.4. The proposed noise reduction methods for digital holograms

As shown in Fig. 3**c**, the GDCT of the digital hologram results in a similar pixel distribution to the original object although the position and the size are somewhat varied. Using this characteristic, this paper proposes a noise reduction algorithm regarding the GDCTed image as the one to apply this algorithm.

3.4.1. Pixel distribution in hologram-domain and DCT-domain

Figure 6 shows positional pixel values of a noise-free CGH and a noisy CGH in both hologram-domain and DCT-domain. First, compare the distribution in the hologram domain (Figs. 6**b** or 6**f**) with the one in the DCT-domain (Figs. 6**d** or 6**h**). It is clear that the two distributions are much different. Also it is easily noticeable that the pixels in DCT-domain are much more correlated than the ones in hologram-domain.

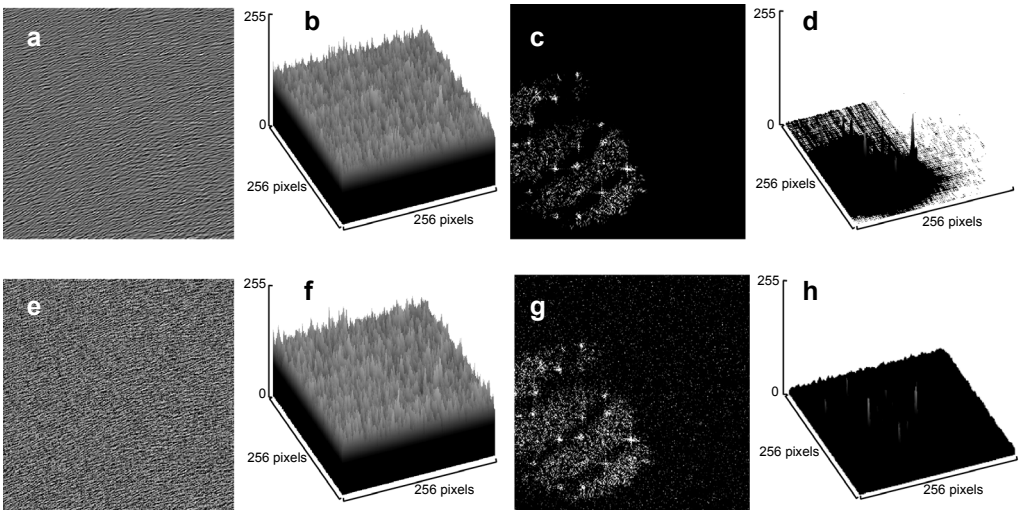

Fig. 6. Pixel distributions in hologram-domain and DCT-domain; noise-free CGH (**a**), positional pixel values of **a** (**b**), GDCTed result of **a** (**c**), positional pixel values of **c** (**d**), noisy CGH by Fig. 4 (**e**), positional pixel values of **e** (**f**), GDCTed result of **e** (**g**), positional pixel values of **g** (**h**).

Now, let us compare the ones of the noise-free CGH and the noisy CGH in which the noise is added by the scheme of Fig. 5. In the hologram-domain the two distributions (Figs. 6**b** and 6**d**) cannot be distinguishable, even their holograms (Figs. 6**a** and 6**c**) look somewhat different. However, the distributions in DCT-domain (Figs. 6**d** and Figs. 6**h**) are quite different in that the pixels in the DCT-domain are much correlated. Especially the pixels inside the objects are relatively highly correlated compared to the ones outside the object. Also, the pixel values outside the object are very small compared to the ones inside the object. It means that the characteristics of the pixels inside the object are much different from the ones outside the object.

Thus, it is more effective to perform the noise reduction in the DCT-domain than in the hologram-domain. Also the object and the background should be separated and different schemes applied to each of the two.

3.4.2. Separating the object from the background

For reasons given in the previous sub-section, we separate the object from the background, whose scheme is shown in Fig. 7. The input of this scheme is the GDCTed image of a noisy CGH. First, an edge detection scheme is applied. In this paper, an algorithm using a gradient is used [14]. Then, it is contoured with a contouring scheme, for which we used the one presented in [14]. Finally, a threshold value is applied to the contoured result to select the pixels larger than the threshold

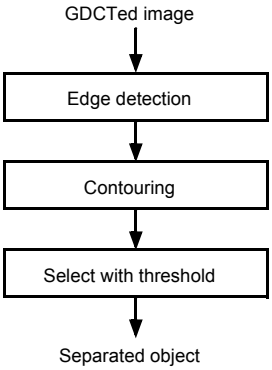

Fig. 7. Object separation scheme.

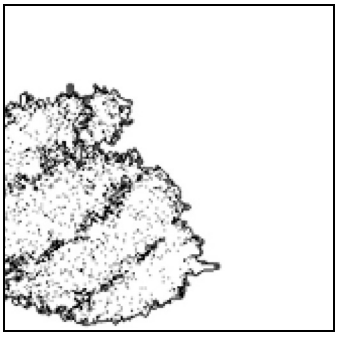

Fig. 8. Example of separated object (threshold = 200).

value, which is found experimentally. One example of the result of applying the object separation scheme to Fig. 7 is shown in Fig. 8, in which the threshold value was 200.

3.4.3. Noise reduction scheme

As mentioned above, we apply different noise reduction schemes for each of the two separated results, object and background. We have tried several schemes to each of the separated regions as in Tab. 1, where each pair of schemes is named as Method 1, Method 2, Method 3, or Method 4. The components of the schemes are as follows.

T a b l e 1. Four noise reduction methods proposed.

Scheme	Object	Background
Method 1	None	Substitution with 0
Method 2	Butterworth low-pass filtering	Substitution with 0
Method 3	Histogram modification	Histogram modification
Method 4	Histogram modification	Substitution with 0

None: no further processing. *Substitution with 0*: this scheme substitutes all the pixels in the region with the ones whose value is 0. *Butterworth low-pass filtering*: butterworth filtering is a well-known method being a kind of weighted average filter with the pixels surrounding a target pixel [15]. *Hologram modification*: The statistical histogram of the pixels of the noisy GDCTed image is somewhat different from that of the noise-free case. To figure out the difference, we have experimented with more than 100 CGHs (refer to Tab. 2) whose original objects are similar to the one in Fig. 3**a**, that is, an object in a background and are of the same size. The resulting histograms of the average noise-free and noisy holograms are shown in Fig. 9, where the horizontal axis and vertical axis represent the pixel value and the frequency, respectively. As can be seen in the figures, the two histograms are apparently different in the mean value and the standard deviation. The purpose of this hologram modification is to remove the portion corresponding to the noise as marked in Fig. 9**b**

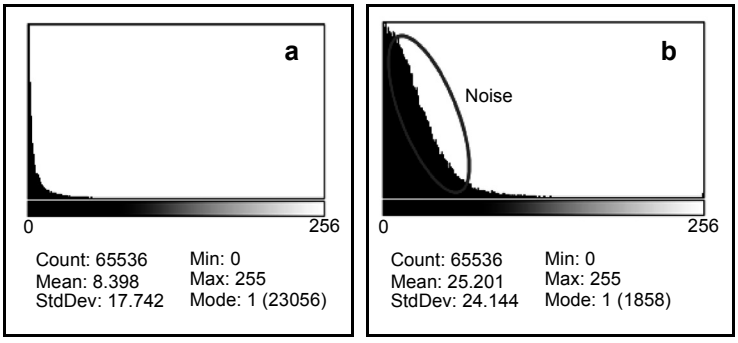

Fig. 9. Average statistical histogram of the digital hologram in the GDCT domain; noise-free case (**a**), noisy case (**b**).

to make a noisy histogram the same as the noise-free one. For this purpose, we used an arithmetic equation:

$$r_s[n] = \begin{cases} \Delta\, h_s[n]\, \dfrac{h_s[n] - C_{\min}}{C_{\max} - C_{\min}} & h_s[n] < 128 \\ 0 & h_s[h] \geq 128 \end{cases} \tag{4}$$

where $r_s[n]$ and $h_s[n]$ are the coefficient values before and after applying the histogram modification technique, respectively; Δ is a weighting factor that is calculated as $18/\sigma$, while σ is the variance of the noisy histogram; $C_{\min}$ and $C_{\max}$ are the minimum and maximum GDCT coefficient values, respectively.

4. Experimental results

4.1. Experimental setup and measurement methodology

The four methods proposed in the previous chapter have been experimented with more than 100 digital holograms (CGHs), as shown in Tab. 2, which consisted of two groups: the ones used generally as the test holograms (*generally used*) and the one we have made (*made by the authors*). The *generally used ones* are the ones used commonly in the previous publications such as rabbit, spring, duck, *etc*. The ones we have made were to provide enough test holograms to get more exact output of the experiments. The method of generating a digital hologram consists in calculating CGH and adding noise as we did in Fig. 5.

T a b l e 2. CGHs used in experiments.

		Applied experiments	
Group	Number	PC simulation	Optical system
Publically used	53	53	12
Made by the authors	49	49	11
total	102	102	23

The methodology of experiment is the same as in Fig. 4, that is, a noisy CGH is first acquired, to which the four noise reduction methods proposed are applied (solid lines in the figure), while the dashed lines are for the performance measures of the proposed methods. Because our target is to improve the quality of the reconstructed holographic image, all the performance measures have been done for the reconstructed images, Fig. 4. We have performed two kinds of reconstructions, PC simulation and optical reconstruction, the parameters of which are given in Tab. 3. For PC simulation, we used *HoloVision* [16], a hologram reconstruction tool by calculation. For optical reconstruction, an apparatus system similar to that of Fig. 1**b** was used which was

T a b l e 3. Parameters of the experimental setup.

Items		PC simulation	Optical system
SLM	Resolution	256×256	1.284×1.024
	Pixel pitch	10.4 μm×10.4 μm	13.62 μm×13.62 μm
Wavelength		633 nm (red)	532 nm (green)
Reconstruction distance		1.000 mm	1.100 mm

an in-line reflective system. The reconstructed images by the optical system were captured with a CCD camera at the imaging position. However, we mainly focused on the PC simulation results because the results from optical system itself include the acquisition noise due to capturing by CCD camera. Thus the image reconstructed by the optical system is only for the visual inspection as auxiliary data. This is also the reason why we used only a part of the test holograms in reconstruction with the optical system as shown in Tab. 3.

To measure the quality of the reconstructed images the PSNR (peak signal to noise ratio) values have been measured using Eq. (5), while the subjective comparison of the image quality has been accomplished with the reconstructed images with optical system as the supporting data

$$\mathrm{PSNR(dB)} = 10 \log \frac{255^2}{\frac{1}{XY}\sum_{x,y}(I_{x,y} - I'_{x,y})^2} \tag{5}$$

Here, $I_{x,y}$ and $I'_{x,y}$ are the values in the position of (x, y) of the noise-free and the noisy reconstructed image, respectively. X and Y are the numbers of pixels in the horizontal and vertical directions in the reconstructed image, respectively.

For the noise signal in Fig. 5, we have performed pre-experiment to determine how much Gaussian noise should be added to meet with the real digital hologram. From this experiment, we obtained the noise level of the camera-captured image corresponding from about 2.5% to about 4.5%. Thus, we have decided to add 5% of the Gaussian noise to a CGH to make the corresponding noisy CGH.

4.2. Results obtained by using a smooth filter

To see how the noise reduction methods for the conventional 2D images work on digital holograms, we have experimented with a smooth filter, which is one of them. As mentioned earlier the experimental results showed that the quality of the reconstructed images after filtering was worse than the one obtained without filtering. One example is shown in Fig. 10, the results being obtained from PC simulation. The PSNR values of the hologram itself of Figs. 10**b** (without filtering) and 10**c** (with filtering) with respect to the noise-free one in Fig. 10**a** were 24.53 dB and 21.53 dB, respectively.

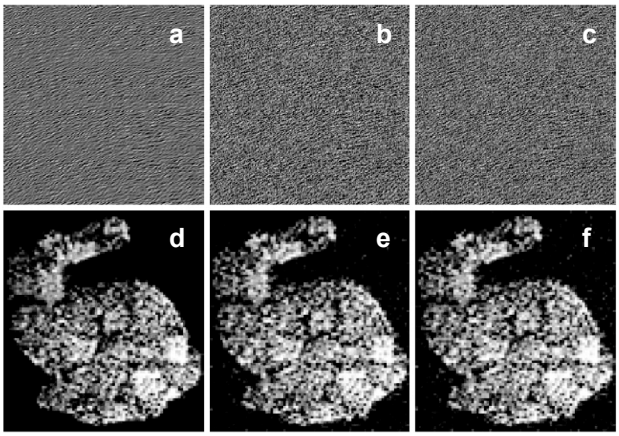

Fig. 10. Digital holograms; original (**a**), noisy (**b**), noise-reduced in the hologram domain by a smoothing filter (**c**), reconstructed images of (**a**), (**b**), and (**c**), respectively (**d**–**f**).

Also the PSNRs of the reconstructed images of Figs. 10**e** and 10**f** to Fig. 10**d** were 21.52 dB and 21.25 dB, respectively. Thus, we can conclude that a mere application of a smoothing filter cannot improve the quality of a noisy digital hologram.

4.3. Results from applying the proposed methods

As mentioned earlier, about 100 test digital holograms were examined by the parameters of *PC simulation* in Tab. 3 and reconstructed by PC simulation. Among them 23 test digital holograms were examined with the parameters of *optical system* and reconstructed by the optical system. The results are shown in Tab. 4 with the average PSNR values and the standard deviations of the four schemes.

As can be seen in Tab. 4, the results from the reconstructed images by the optical system were worse than the ones by PC simulation (lower PSNR average and larger standard deviation) because the image captured with a CCD camera by the optical system incorporates some acquisition noise. But in both reconstruction methods, all the four methods proposed showed more or less improved results after applying the methods. Among them Method 4 showed the best performance with improvement of 6.12 dB in PSNR value for the *PC simulation*.

T a b l e 4. Improvement of image quality by the methods proposed.

			Noise-reduced hologram			
	Noisy hologram		PC simulation		Optical system	
Method	PSNR	σ^2	PSNR	σ^2	PSNR	σ^2
Method 1	24.35dB	1.35	26.55dB	1.48	25.32	1.89
Method 2	24.35dB	1.35	26.75dB	1.30	25.51	1.53
Method 3	24.35dB	1.35	29.63dB	1.12	28.39	1.44
Method 4	24.35dB	1.35	30.47dB	1.13	29.23	1.46

By examining the data in Tab. 4, it is noticeable that the proposed histogram modification scheme works very well for the objects as in Method 3 and Method 4. But for the background the substitution with 0 scheme turned out to be better than the histogram modification scheme.

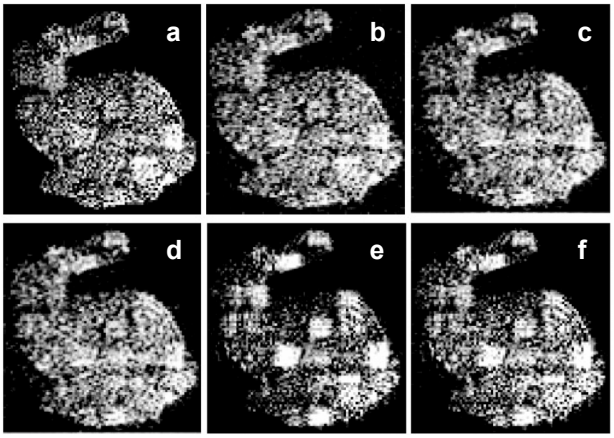

Fig. 11. Reconstructed images using PC: original (**a**), noisy (**b**), Method 1 (**c**), Method 2 (**d**), Method 3 (**e**), Method 4 (**f**).

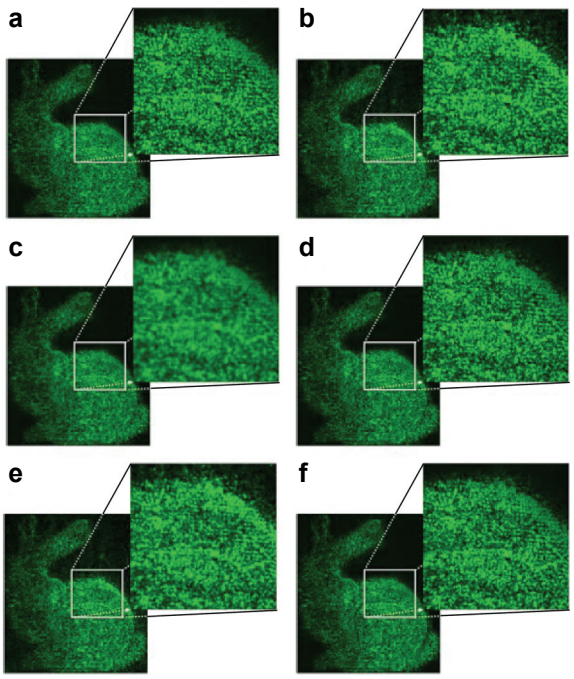

Fig. 12. Reconstructed images using an optical system: original (**a**), noisy (**b**), Method 1 (**c**), Method 2 (**d**), Method 3 (**e**), Method 4 (**f**).

Figure 11 shows an example of experimental results by the PC simulation. The visual examination could also prove that the qualities in Figs. 11**c**, 11**d**, 11**e**, and 11**f** are better than that of 11**b** and the results from Method 4 is best visually as well as numerically as Tab. 4 shows. In Figure 12, the experimental results of the same test hologram as in Fig. 11 by the optical reconstruction are presented. Of course, its parameters were the same as the ones of *optical system* in Tab. 3. Overall image qualities of them are better than the ones in Fig. 11 because the hologram resolutions for the optical system were more than 4 times higher than the ones for the PC simulation. By visual inspection, it is obvious that all the methods proposed improve the quality of image reconstructed by the optical system as well. And the result from Method 4 is the best.

Consequently, it can be said that all the proposed methods improve the image quality in both numerical value and visual inspection, being in both cases reconstructed by *PC simulation* and optical system. Also, the method with the histogram modification scheme for the object and the substitution with 0 scheme for the background is the best choice to reduce the noise.

5. Conclusions

This paper assumes that a digital hologram is obtained by capturing the interference pattern with a CCD camera, which is one of the common methods. Because of using a CCD camera, the captured image usually includes quite a lot of noise due to the characteristics of the camera. This noise is one of the major causes of the decreased quality of reconstructed image and this paper is aiming at this issue.

This paper proposed algorithms to reduce noise added during the acquisition and transmission process of a digital hologram. These algorithms are applied to the data in the frequency-domain transformed by 2DGDCT. First, it separates the object from the background data. For each of the two separated parts, different noise scheme is applied and we proposed four types of such scheme-pairs.

Experimental results showed that the technique of reducing noise in a conventional 2D image such as a smoothing filter could not reduce the noise to improve the image quality for a digital hologram. But by applying our methods, the image qualities for all of the four cases were improved by at least 2.2 dB in the PSNR average. Especially, Method 4 that applied the histogram modification for the object and substituted the background with the pixels valued as 0 worked the best – the PSNR improvement was greater than 6.12 dB.

The four kinds of the proposed noise reduction methods are therefore expected to be practical base technologies in the image communication industry for digital holography such as holographic TV, next generation 3D realistic TV, *etc*.

Acknowledgements – This work was supported by the Seoul Development Institute funded by the Seoul R&BD(NT080528) Program.

References

[1] MATOBA O., NAUGHTON T.J., FRAUEL Y., BERTAUX N., JAVIDI B., *Three-dimensional object reconstruction using phase-only information from a digital hologram*, Proceedings of SPIE **4864**, 2002, pp. 122–128.

[2] JAVIDI B., OKANO F., *Three Dimensional Television, Video, and Display Technologies*, Springer Verlag, Berlin, 2002.

[3] SHORTT A.E., NAUGHTON T.J., JAVIDI B., *A companding approach for nonuniform quantization of digital holograms of three-dimensional objects*, Optics Express **14**(12), 2006, pp. 5129–5134.

[4] CAI X., WANG H., *Study of relationship between recording wavelength and hologram compression*, Optics Communications **265**(1), 2006, pp. 111–115.

[5] WIDJAJA J., *Objective evaluation of information retrieved from digitally compressed in-line holograms*, Optics and Lasers in Engineering **44**(12), 2006, pp. 1239–1251.

[6] DARAKIS E., SORAGHAN J.J., *Use of Fresnelets for phase-shifting digital hologram compression*, IEEE Transactions on Image Processing **15**(12), 2006, pp. 3804–3811.

[7] DARAKIS E., SORAGHAN J.J., *Reconstruction domain compression of phase-shifting digital holograms*, Applied Optics **46**(3), 2007, pp. 351–356.

[8] GARCIA-SUCERQUIA J., RAMIREZ J.A.H., PRIETO D.V., *Reduction of speckle noise in digital holography by using digital image processing*, Optik – International Journal for Light and Electron Optics **116**(1), 2005, pp. 44–48.

[9] CAI X., WANG H., *The influence of hologram aperture on speckle noise in the reconstructed image of digital holography and its reduction*, Optics Communications **281**(2), 2008, pp. 232–237.

[10] LIN L.C., *An error detection and recovery algorithm for the transmission of digital holography over noisy channels*, Optics Communications **281**(5), 2008, pp. 1008–1016.

[11] SHARMA A., SHEORAN G., MOINUDDIN JAFFERY Z.A., MOINUDDIN, *Improvement of signal-to-noise ratio in digital holography using wavelet transform*, Optics and Lasers in Engineering **46**(1), 2008, pp. 42–47.

[12] SEO Y.-H., CHOI H.-J., KIM D.-W., *Lossy coding technique for digital holographic signal*, Optical Engineering **45**(6), 2006, p. 065802.

[13] ITO T., MASUDA N., YOSHIMURA K., SHIRAKI A., SHIMOBABA T., SUGIE T., *Special-purpose computer HORN-5 for a real-time electroholography*, Optics Express **13**(6), 2005, pp. 1923–1932.

[14] GONZALES R.C., WOODS R.E., *Digital Image Processing*, 3rd Edition, Pearson Prentice Hall, Upper Saddle River, NJ, 2008.

[15] LEE J.-S., *Digital image smoothing and the sigma filter*, Computer Graphics and Image Processing **24**(2), 1983, pp. 255–269.

[16] http://www2.edge.no/projects/index.php?expn=2&target=holovision/about.php.

Received October 13, 2010
in revised form February 22, 2010